The Attainable Gravimetric and Volumetric Energy Density of Li-S and Li-Ion Battery Cells with Solid Separator-Protected Li-Metal Anodes

Bryan D. McCloskey[1,2]
[1]*Department of Chemical and Biomolecular Engineering, University of California, Berkeley, CA, 94720*
[2]*Environmental Energy Technologies Division, Lawrence Berkeley National Laboratory, Berkeley, CA, 94720*

Supporting Information

A note on the calculations provided in the Excel spreadsheet. 6 spreadsheets are available to calculate the gravimetric and volumetric energy density of the cells studied. All red numbers in the spreadsheet are adjustable parameters. The goal seek tool in Excel was used to calculate many of the values provided in the main text (e.g., values in Table 1 and 2). For example, to calculate the first sulfur loading value in Table 1 (2.4 mg/cm^2), the cell parameters listed in Table S6 were input into the 'Elyte-to-S' spreadsheet, along with the cathode composition listed in the Table 1 caption and left hand column, and a goal seek was used on cell J25, the cell specific energy, setting its value to 268 by changing cell A25, the sulfur loading.

Table S1. Densities (g/cm^3) for all materials that comprise the batteries in this study. LLZO, LATP, and LPS values from [1-3].

Li metal	0.534
Li-ion cathode active material	4.4
Sulfur	2.07
Carbon/graphite	2.2
Binder	1.76
Liquid electrolyte	1.1
Al CC	2.7
Cu CC	9
Polypropylene (PP)	0.95
$Li_7La_3Zr_2O_{12}$ (LLZO)	5.1
$Li_{1+x}Al_xTi_{2-x}(PO_4)_3$ (LATP)	3.0
Li_2S-P_2S_5 glasses (LPS)	1.88

Parameters for figures and tables in the main text are provided in the tables below. All cells, both Li-ion and Li-S, employ a 10 μm Al current collector, a 4 μm Cu anode current collector. The Li-ion battery cathode has properties listed in Figure 1 in the main text.

Table S2. Figure 2-5 Graphite-based anode Li-ion (LIB (C)) parameters. Cathode properties provided in Fig. 1 in the main text, although the active cathode material loading was varied in Fig. 2b and 5. Dry density and porosity were calculated from graphite/electrolyte wt ratio (i.e., they are not input parameters).

Anode/cathode capacity ratio	1.2	
Graphite/electrolyte in anode wt ratio	6	
Binder in anode	5	wt%
Dry anode density	1.65	g/cm^3
Anode porosity	24	vol%
Anode capacity	330	mAh/g
PP separator thickness	25	μm
PP separator porosity	55	vol%
Average cell operating voltage	3.6	V

Table S3. Figure 3-4 Li metal-based anode Li-ion (LIB (Li)) input parameters. Cathode properties provided in Figure 1d in the main text.

Li metal excess	20	%
LATP separator thickness	40	μm
Average cell operating voltage	3.7	V

Table S4. Figure 3 Li-S input parameters.

Carbon wt% in cathode	0	%
Binder wt% in cathode	0	%
Li metal excess	20	%
LATP separator thickness	40	μm
Average operating voltage	2.2	V
S utilization	100	%

Table S5. Figure 4 and 5 Li-S input parameters.

Carbon wt% in cathode	20	%
Binder wt% in cathode	5	%
Li metal excess	20	%
LATP separator thickness	40	μm
Average operating voltage	2.0	V
S utilization	60	%

Table S6. Table 1 Li-S input parameters.

Binder wt% in cathode	5	%
Li metal excess	20	%
LATP separator thickness	40	μm
S utilization	1250	mAh/g
Average operating voltage	2.2	V
E/S ratio	1	μL/mg

Table S7. Table 2 Li-S input parameters.

Carbon wt% in cathode	20	%
Binder wt% in cathode	5	%
Li metal excess	20	%
LATP separator thickness	40	μm
Average operating voltage	2.0	V
Total electrolyte volume	30	$\mu L/cm^2$

Description of Figure 5. A simple cost analysis was performed to calculate the material costs per kWh. These calculations only included the cell components shown in Figure 1a-c and do not include the cell housing or provide a pack-level analysis. However, as was stated in the main text, we expect cell housing and pack level components to be reasonably similar between Li-ion and Li-S batteries, such that the primary difference in battery cost will be influenced by differences in cell components and assembly. The assembly cost of cells employing protected Li metal anodes is unknown, but likely to be higher than assembly costs of graphite anode-based cells with a polymer separator. I give Li metal cells the benefit of the doubt in this respect and assume that assembly costs of graphite and Li metal-based cells will be equal, thereby making the difference in cell costs entirely related to materials costs. Equation S1 was used to calculate the material costs per kWh of the cells shown in Figure 6:

$$P_T = \frac{\sum \varepsilon_i m_i + \sum c_j}{V \cdot m_A \cdot C} \qquad \text{(S1)}$$

P_T = Total cost per kWh of all cell components ($/kWh)
ε_i = Cost of component '*i*' ($/g)
m_i = Mass loading of component '*i*' (g/cm^2); where *i*= carbon, binder, active material electrolyte, Li metal
c_j = Cost per area of component '*j*' ($/cm^2); where *j*= current collectors, separator
V = Average cell operating voltage (V)
m_A = Active cathode material loading (g/cm^2)
C = Active material capacity (kAh/g)

The active material loading of both Li-ion and Li-S batteries (at a constant Li or graphite capacity excess of 20%) is varied in Figure 5 to probe different specific energies. The component costs used in the cost estimate are provided in Table S8 and were selected from values provided by Nelson et al.[4]

Table S8. Cost for cell materials. The solid separator cost is used as an adjustable parameter and therefore not included here.

Li metal	0.05	$/g
NCA	0.037	$/g
S	0.00022	$/g
Anode C	0.019	$/g
Cathode C	0.006	$/g
Binder	0.01	$/g
Electrolyte	0.018	$/g
Al CC	0.00008	$/cm^2
Cu CC	0.00018	$/cm^2
PP separator	0.0002	$/cm^2

Comparison of graphite anode-based Li-S and LIB (C) cells

Figure S1 compares the energy density of Li-ion and Li-S cells employing graphite anodes. In this comparison, both cells are identical except for their cathode composition, having cell geometries similar to what is shown in Fig. 1a (with the Li-S cell obviously employing a S cathode rather than the NCA cathode in Fig. 1a). The Li-S cell studied in Fig. S1a has a cathode composition described in Table S4, and the cathode used in Fig. S1b is described in Table S5.

When comparing the results of Fig. S1 to analogous Li-metal anode-based Li-S cells in Fig. 3 and 4, significantly smaller E/S ratios are clearly required for graphite anode-based Li-S cells to achieve comparable energy densities to Li-metal-based cells employing 40 μm separators. For example, for the 'realistic' cells studied in Fig. S1b and 4a to compete with a state-of-the-art LIB (C) cell on a gravimetric energy density basis, the maximum allowable E/S ratio (at infinite sulfur loading) decreases from 5.3 for the Li-metal-based cell to 1.5 for the graphite-based cell. On a volumetric basis, the maximum possible E/S ratio calculated for the 'realistic' graphite-based cell to compete with a LIB (C) cell is ~0.05 (not plotted). At more realistic S loadings (e.g., <5 mg/cm²), the maximum E/S ratio drops to below 0.25, as is observed in Fig. S1b.

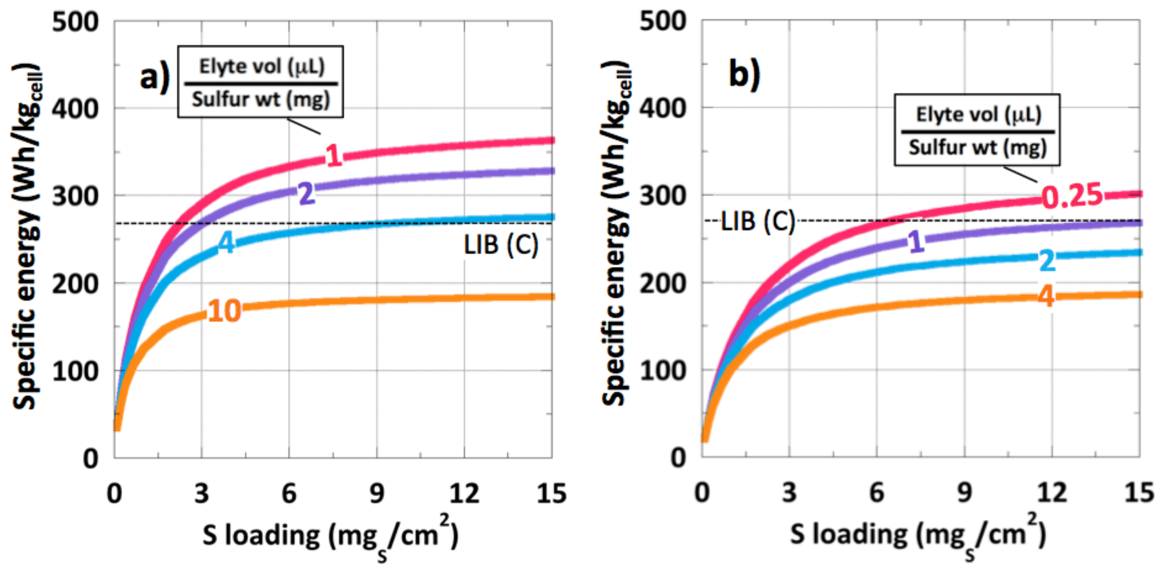

Figure S1. Comparison of energy densities of Li-S and Li-ion batteries employing graphite anodes. a) Comparison of a baseline LIB(C) cell with an 'ideal' Li-S cell (100% S cathode, 100% S utilization, 2.2V operating potential). b) Comparison of a baseline LIB(C) cell with a 'realistic' Li-S cell (75% S cathode, 60% S utilization, 2.0V operating potential). A 25 μm electrolyte-wetted separator was used in all cells. The E/S ratio is calculated only using the weight of the electrolyte wetting the cathode (does not include electrolyte wetting the anode or the separator).

References

(1) Cheng, L.; Chen, W.; Kunz, M.; Persson, K.; Tamura, N.; Chen, G.; Doeff, M. Effect of surface microstructure on electrochemical performance of garnet solid electrolytes. *ACS Appl. Mater. Interfaces* **2015**, *7*, 2073-2081.

(2) Christensen, J.; Albertus, P.; Sanchez-Carrera, R. S.; Lohmann, T.; Kozinsky, B.; Liedtke, R.; Ahmed, J.; Kojic, A. A critical review of Li/air batteries. *J. Electrochem. Soc.* **2012**, *159*, R1-R30.

(3) Prasada Rao, R.; Adams, S. N.; Reddy, M. V.; Chowdari, B. V. R. Li+ conductivity and migration pathway studies of LiCl doped $0.6Li_2S$-$0.4P_2S_5$ glassy electrolyte for all-solid-state batteries *Meeting Abstracts, 15th IMLB* **2010**, 185.

(4) Nelson, P. A.; Gallagher, K. G.; Bloom, I.; Dees, D. W. Modeling the performance and cost of lithium-ion batteries for electric-drive vehicles, second edition, Argonne National Laboratory Report ANL-12/55. **2012**.